

An X-ray polarimeter for hard X-ray optics

Fabio Muleri^a, Ronaldo Bellazzini^b, Enrico Costa^a, Paolo Soffitta^a, Francesco Lazzarotto^a, Marco Feroci^a, Luigi Pacciani^a, Alda Rubini^a, Ennio Morelli^c, Luca Baldini^b, Francesco Bitti^b, Alessandro Brez^b, Francesco Cavalca^b, Luca Latronico^b, Marco Maria Massai^b, Nicola Omodei^b, Michele Pinchera^b, Carmelo Sgró^b, Gloria Spandre^b, Giorgio Matt^d, Giuseppe Cesare Perola^d, Oberto Citterio^e, Giovanni Pareschi^e, Vincenzo Cotroneo^e, Daniele Spiga^e, Rodolfo Canestrari^e

^a Istituto di Astrofisica Spaziale e Fisica Cosmica, Via del Fosso del Cavaliere 100, I-00133 Roma, Italy;

^b Istituto Nazionale di Fisica Nucleare, Largo B. Pontecorvo 3, I-56127 Pisa, Italy

^c Istituto di Astrofisica Spaziale e Fisica Cosmica, Via Gobetti 101, I-40129 Bologna, Italy

^d Università degli Studi di Roma 3, via della Vasca Navale 84, I-00146 Roma, Italy

^e Osservatorio Astronomico di Brera, via E. Bianchi 46, I-23807 Merate (LC), Italy

ABSTRACT

Development of multi-layer optics makes feasible the use of X-ray telescope at energy up to 60-80 keV: in this paper we discuss the extension of photoelectric polarimeter based on Micro Pattern Gas Chamber to high energy X-rays. We calculated the sensitivity with Neon and Argon based mixtures at high pressure with thick absorption gap: placing the MPGC at focus of a next generation multi-layer optics, galactic and extragalactic X-ray polarimetry can be done up till 30 keV.

Keywords: Hard X-rays, telescopes, Polarimetry

1. INTRODUCTION

1.1. Hard X-Ray Telescopes

In the History of X-ray Astronomy a crucial turning point was the introduction of X-ray Optics, first aboard some rockets and eventually on satellite with the HEAO-2/Einstein mission. Optics play two major functions:

- to image a field of X-ray Sky, to study extended sources, to resolve nearby sources, to localize sources with high angular accuracy;
- to increase dramatically the signal to noise ratio, also with respect to other imaging systems, such as coded masks or modulation collimators. A source is to be compared with the fluctuations of background inside the point spread function of the telescope and not with the total background of the detector.

This tremendous power of X-ray optics has been originally applied to softer X-rays with Einstein and ROSAT, and has been extended to higher energies to include the Fe lines region, with ASCA, SAX, Newton and Chandra. The conventional X-ray optics are limited in band because of the intrinsic limits set by the laws of total reflection. The critical angle of reflection is roughly proportional to the square root of the density of the reflecting material and to the wavelength of the photons. Thence, as the margin of increase in density, with respect to gold, is very limited, the extension to higher energies is committed to inner shells with progressively smaller projected area. The extension to higher energies is therefore paid with a large number of shells and with a proportional reduction of the field of view. Historically the X-ray telescopes have been used up to 10 keV. Some extended

Further author information: (Send correspondence to Fabio Muleri)

Fabio Muleri: E-mail: Fabio.Muleri@iasf-roma.inaf.it, Telephone: +39-0649934565

capabilities of Newton at higher energies have not been effective because of an area mismatched with that at lower energies and because of a high background due to the large plate-scale.

In the future the revolution of the application of optics is about to be extended to higher energies, thanks to the use of telescopes with multi-layer coatings,¹ alternating layers of high Z and low Z materials of gradually changing thickness. This technique provides effective reflection at angles up to 3 times those of mono-layer surfaces and makes feasible telescopes effective up to 60-80 keV (in practice up to the K absorption edge of the high Z reflecting material). At lower energies they are not as good as conventional optics, due to the photoelectric absorption of the high Z component, but an improvement could be the recently proposal of over-coating the multilayer surface with a carbon layer.² New missions based on the concept of multilayer telescopes have been proposed and NUSTAR and SIMBOL-X have passed a certain level of selection. Depending on various constructive parameters these missions can gain from two to three orders of magnitude in sensitivity with respect to the best previous experiments based on collimation (PDS) or coded mask (IBIS). Also future big telescopes for X-ray Astronomy, such as NEXT, CON-X or XEUS should include such optics. The science to be performed with these telescopes is mainly based on spectroscopy (cyclotron lines, hard tails, Compton-thick objects etc.). Also imaging can play a role. E.g. the Diffuse X-ray Background peaks around 40 keV. A hard X-ray telescope could resolve the large majority of it into discrete sources. Moreover imaging of extended objects with hard non-thermal components, such as some Super Nova Remnants and some Galaxy Clusters, could help to localize the hard emission and correlate it to the dynamics of the system.

1.2. X-Ray Polarimetry

In this paper we want to discuss another point: the capability to perform Polarimetry of X-ray Sources in the Hard X-ray Band and the benefit to employ multi-layer optics for this purpose.

Since the birth of X-ray Astronomy, theoretical analysis has suggested that measuring the linear polarization of X-rays could significantly improve our knowledge of Physical Processes and of geometry of regions of the source emitting X-rays and its transfer toward the observer.

Here the question rises whether the extension to higher energies is only a matter of completeness or, on the contrary, a specific science is there that can only be performed at best at higher energies. We try to lay down a few hot topics of High Energy Astrophysics, for which the polarimetry at higher energies would be more easy or more significant.

- X-ray pulsator, resonance frequency, inversion of the polarization plane (normal - anomalous), higher polarization;
- polarization by scattering on disks: LMXRB, QSO, Seyfert-1;
- non thermal components in extended objects: SNR, Clusters out of the thermal component;
- effects of GR on disks: Cyg X-1, AGN (increasing effects closer to the inner orbits);
- blazars: transition from synchrotron to inverse Compton.

From these items it is apparent the strong interest to extend the measurements of polarization to hard X-rays. Is this feasible?

The conventional approach to X-ray polarimetry includes two major techniques:

- Bragg Diffraction at 45° . It provides an excellent response to the polarization, conventionally expressed with a modulation factor μ close to 1. Conversely the overall efficiency of the process is very poor because only the photons within a narrow band around the angle that satisfies the Bragg condition are reflected. The efficiency can be increased by the use of mosaic crystals providing a larger band-pass.

- Compton scattering. It provides a good analyzer of the linear polarization if the system is designed in such a way to limit the scattering angles around 90° . Since the scattered photons will be distributed in angle according to the Klein-Nishina cross section, this will automatically limit the efficiency of the instrument. The optimal sensitivity will derive from a trade-off on the acceptance angles. At low energies, when the energy lost in the scattering is low, the scatterer must be a passive low Z material, usually Lithium, encased in a thin beryllium can, to give mechanical consistency and to prevent oxidation or nitridation. This device loses the imaging properties of the optics and is background dominated. If the scatterer is not geometrically perfect and if the pointing does not keep the beam exactly on the axis of the scatterer, huge spurious polarizations are generated. At higher energies an active scatterer can be used, such as a detector based on plastic scintillator or, at even more high energies, on silicon. Such a device could be in principle position sensitive. But the active scattering polarimeters built so far never arrived below 50 keV. Active scatterers based on Silicon will be likely operative at energies even higher.

Bragg diffraction allowed the first and till now unique measure of X-ray polarization from an astronomical source: the polarimeter on board OSO-8 satellite, observing Crab Nebula for 3 days, succeeded to detect a polarization of $19.22 \pm 0.92\%$ at 2.6 and 5.2 keV aligned with optical polarization.³ This confirmed that X-ray emission is due to synchrotron process, the same as other wavelengths.

Bragg diffraction and Compton scattering, in a focal plane version, were employed at best in the Stellar X-Ray Polarimeter.⁴ A thin pyrolytic graphite crystal was set above the focal plane to reflect (diffract) photons and to convey them to a detector on a *secondary* focal plane. The rotation of the whole would modulate the diffracted flux according to the amount and angle of polarization of the photons. The higher energy photons would pass the graphite, impinge on a lithium stick. Four detectors all around in a well configuration would detect scattered photons. SXP was supposed to fly aboard the SRG Mission, that was never completed. But notwithstanding the huge SODART optics it would be dominated by the background at source level of a fraction of Crab.

2. THE MICROPATTERN DETECTOR

The relatively recent discovery of device capable to measure the linear polarization of X-rays by means of the angular distribution of photoelectrons provides an alternative. The Micropattern Gas Chamber^{5,6,7} has excellent imaging properties, is relatively broad band with an energy resolution suitable for continua and photons can be tagged with time at μsec level.

The recent development of ASIC chips including anode pads and a complete Front End Electronics make this device very compact and easy. The MPGC is discussed in other papers in this same book (see ref. 6 and ref. 7). We discuss here how and how much the technique can be applied in the Hard X-Ray range, covered by multi-layer optics. Our considerations are mainly based on computations and simulations.

The major adaptation of the MPGC for applications on Hard X-Rays is the change of the gas mixture in composition and pressure and the change in the thickness of the absorption/drift gap. We stress the point that the simulations performed here are based on the same programs we use at lower energies. This extension is very reliable because we are using equations and tabulations in a range where they are even better determined.

We discuss the performance and the optimization of our detector combining its response with that of the optics. As a bench-mark optics for our simulations we use three of the various designs of SIMBOL-X mission, described in tab.1. In fig.1 we indicate the effective area of the telescope alone.

As to the detector we assume the last generation of the ASIC chip of 105k pixel at $50\mu\text{m}$ pitch (see ref. 6 and ref. 7) and let free to vary the thickness of the absorption gap and mixture pressure. We considered Neon and Argon based mixtures with a small percentage of DME (20% and 40% respectively).

As to the filling mixture we can fix some general principles:

- To increase the efficiency ϵ and extending at higher energy MPGC technique, filling gas of higher atomic number or higher pressure should be used;

Table 1. Main features of the telescopes used as a bench-mark.

	Design 1	Design 3	Design 4
Focal lenght (m)	20	25	30
Max diameter (cm)	70	70	70
Weight (kg)	215	229	239
FoV (arcmin)	12.7	10.9	9.2
FoV area (arcmin ²)	161.6	118.5	85.2

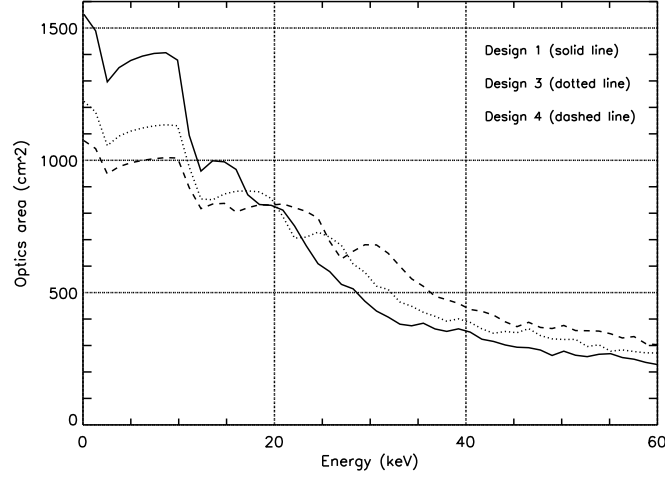


Figure 1. Area vs energy dependence of three different SIMBOL-X design.

- Modulation μ is larger for low pressure or low Z mixture;
- Increasing thickness of the absorption gap implies an efficiency increase but a modulation decrease.

Since sensitivity, expressed as a Minimum Detectable Polarization (MDP), is inversely proportional to $\mu\sqrt{\epsilon A}$ where A is optics area, we need a trade-off between efficiency and modulation in telescope band-pass.

2.1. Sensitivity calculation

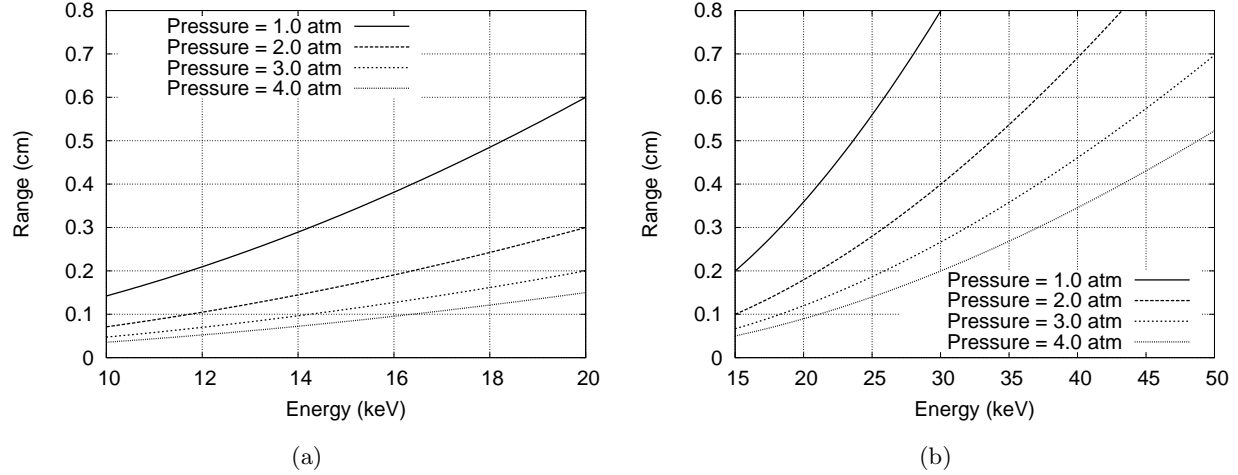
Modulation factor for each mixture was calculated from simulating photoelectric absorption, photoelectron propagation and charge collection in the mixture.⁸ Absorption from K and L shells was considered, assuming for energy larger than K edge the subshells cross section ratio and 2-p asymmetry parameter at K edge. In tab. 2 we report subshell emission probability and the 2-p asymmetry parameter at K edge for some mixture elements: only a small fraction of photons are absorbed by 2-p subshell which is not completely modulated.

We calculated modulation factor at a given energy simulating absorption of 25000 photons which are directed orthogonally respect to ASIC chip. The optics focusing on detector skew direction of photons up till angle $\sim 3^\circ$: simulations suggest that the only effect is a slightly decreasing of the modulation factor.

Only photoelectrons which were completely absorbed in mixture are considered: so the energy range is upper limited such that the photoelectron range is less than the chip dimensions (about $15 \times 15 \text{ mm}^2$). In fig. 2(a) and fig. 2(b) we report the approximate electron range dependence for Ne and Ar based mixtures at different pressure to give a raw upper limit to the MP GC extension at high energy.

Table 2. Subshell emission probability and the 2-p asymmetry parameter for some mixture elements.⁹

Element	K edge (keV)	P_{1s}	P_{2s}	P_{2p}	Asymmetry parameter
C	0.284	95.2%	4.2%	0.6%	0.958
O	0.543	94.1%	4.3%	1.6%	0.955
Ne	0.870	93.3%	4.2%	2.5%	0.955
Ar	3.206	92.0%	5.1%	2.9%	0.820

**Figure 2.** Approximate electron range dependence for Ne 80% + DME 20% (a) and Ar 60% + DME 40% mixture (b).

The energy lower limit for Ne and Ar based mixtures was about twice K shell edge because photoelectron emission is often followed by Auger electron production: if its energy is larger than that of the photoelectron, standard reconstruction algorithm may fail in track analysis. In tab. 3 we report K edge energy and fluorescence yield for some mixture elements.

The MPGC energy upper limit can be overcome by using mixtures based on higher Z element, such as Krypton or Xenon: in this case the high probability of fluorescence produces a certain number of combinations of low energy electrons that does not allow the straightforward approach we followed so far. We are still investigating this issue.

Table 3. K shell edge and fluorescence yield for some elements.¹⁰

Element	K edge (keV)	Fluorescence yield K	Fluorescence yield L
C	0.284	0.26%	negligible
O	0.543	0.69%	negligible
Ne	0.870	1.50%	negligible
Ar	3.206	12.0%	~0.02%
Kr	14.33	65.2%	~2.0%
Xe	34.59	88.8%	~8.0%

All the set of data are analysed in sensitivity calculation: however we already know that cuts on track shape would increase modulation factor. This would imply an efficiency decrease and so the cuts must be fitted very well with every mixture to ensure the best MDP.

2.1.1. High Pressure Neon Mixtures

A baseline solution is to use mixtures based on high pressure Ne with thick absorption gap. Computations involve mixtures of 80% of Neon and DME at 1 atm, 2 atm 3 atm and 4 atm pressure and 1 cm, 2 cm, 3 cm absorption gap thickness.

In fig. 3(a), 3(c) and 3(e) we plotted modulation factor vs energy dependence for each mixture analysed. The factor $\mu\sqrt{\epsilon}$, which is an optics independent sensitivity estimate, is reported in fig. 3(b), 3(d) and 3(f). End of the curves indicate photon energy at which charges, generated by photoelectron and amplified from GEM, are collected out of ASIC chip.

Increasing mixture pressure and absorption gap thickness allows to reach higher peak sensitivity and larger energy band, both shifted at higher energy. For example, a 2 atm pressure mixture with an absorption gap thickness of 1 cm is sensitive above 3 keV (modulation greater than $\sim 10\%$) up till 25 keV, peaking at about 5 keV, while sensitivity of a 4 atm 3 cm mixture peaks at 8 keV and is very high from 4 keV up till 25 keV.

2.1.2. Argon Mixtures

We repeated sensitivity calculations for Ar 60% + DME 40% at 1 atm, 2 atm 3 atm and 4 atm pressure with 1 cm, 2 cm and 3 cm: results are reported in fig. 4.

The modulation factor (fig. 4(a), 4(c) and 4(e)) does not decrease significantly if mixture pressure or absorption gap thickness are increased: this allows to reach high sensitivity even at very high energy without a significant modulation reduction. Sensitivity is higher than Neon based mixtures and energy band is larger, balancing the intrinsic lower fluxes from astronomical sources at high energy.

3. DISCUSSION

The sensitivity curves presented in fig. 3 and 4 prove that MPGC can be easily adapted to hard X-ray polarimetry. Of particular interest is the possibility of tuning the instrument to the optics: choosing Neon or Argon based mixture, a suitable pressure and absorption gap thickness, the best sensitivity can be shifted into the telescope band-pass.

A Neon based mixture at intermediate pressure and absorption gas thickness provides good modulation factor even at lower energy where sources fluxes are larger. For example, MPGC filled with a mixture of 80% of Neon and DME at 2 atm pressure and 2 cm gap thickness provides a good sensitivity above 4 keV up till 15 keV. Polarimetry at higher energy can be performed by filling MPGC with Argon based mixtures.

A better scientific knowledge would be reached in a two telescope mission with two MPGC filled with Neon and Argon based mixtures: in this configuration X-ray polarization could be measured in different energy bands. This would provide a deeper understand of astronomical X-ray sources because emission and transport processes change radiation polarization with energy. The low energy MPGC could be filled with Neon at low pressure with an high component of DME to reduced diffusion of photoelectrons and secondary charges or with another suitable mixture (like DME + He, which is sensitive above 2 keV up till ~ 10 keV, see ref. 11), while the high energy specialized MPGC could be filled with an Argon based mixture at high pressure and high gap thickness. For example, sensitivity of Argon 60% + DME 40% mixture at 3 atm pressure and 3 cm gap thickness peaks at 12 keV and remains significant till 30 keV*.

*Better sensitivity can be reached with mixture at 4 atm pressure, but gas discharges prevent to obtain high gain in GEM charge multiplication.

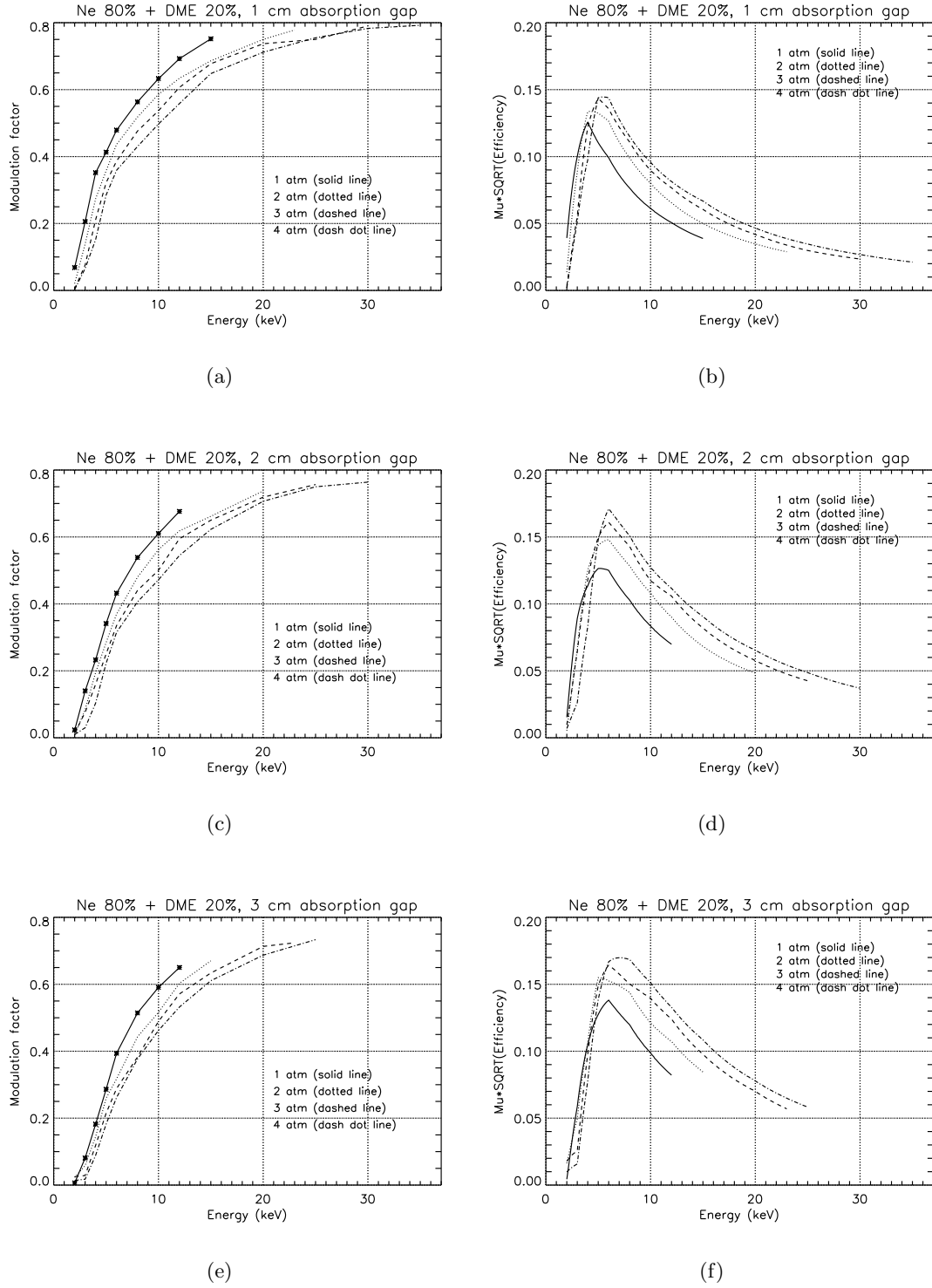
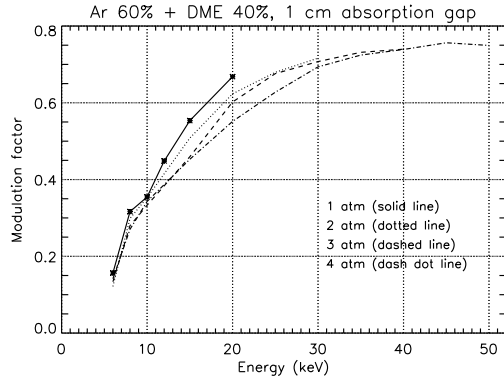
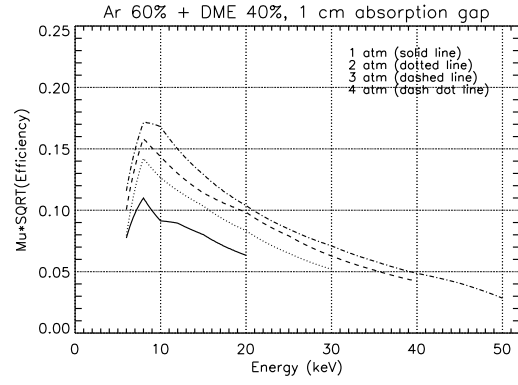


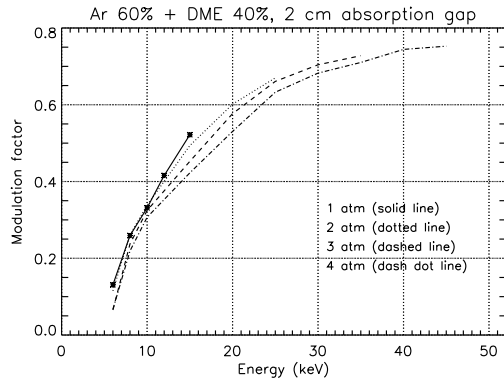
Figure 3. Modulation (a, c and e) and sensitivity factor $\mu\sqrt{\epsilon}$ (b, d and f) vs photon energy for Ne 80% + DME 20% mixture with 1 cm, 2 cm and 3 cm absorption gap thickness respectively. Curves end indicates energy at which secondary charges are collected out of ASIC chip. Efficiency includes a 50 μm beryllium window.



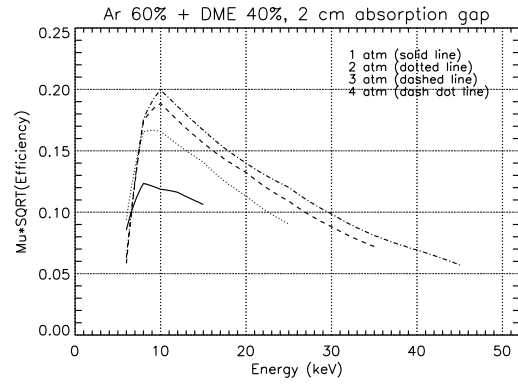
(a)



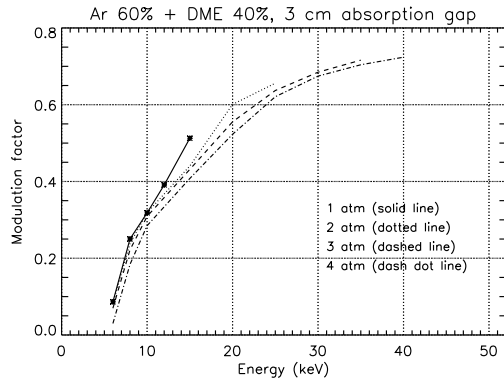
(b)



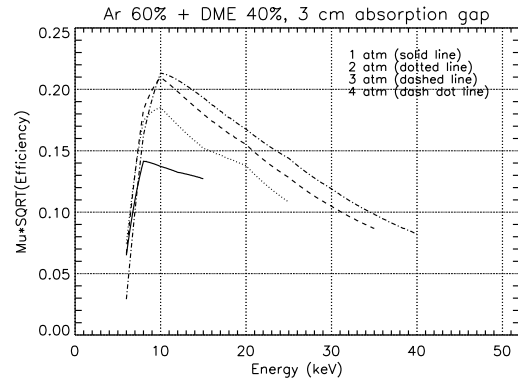
(c)



(d)



(e)



(f)

Figure 4. Modulation (a, c and e) and sensitivity factor $\mu\sqrt{\epsilon}$ (b, d and f) vs photon energy for Ar 60% + DME 40% mixture with 1 cm, 2 cm and 3 cm absorption gap thickness respectively. Curves end indicate energy at which secondary charges are collected out of ASIC chip. Efficiency includes a 50 μm beryllium window.

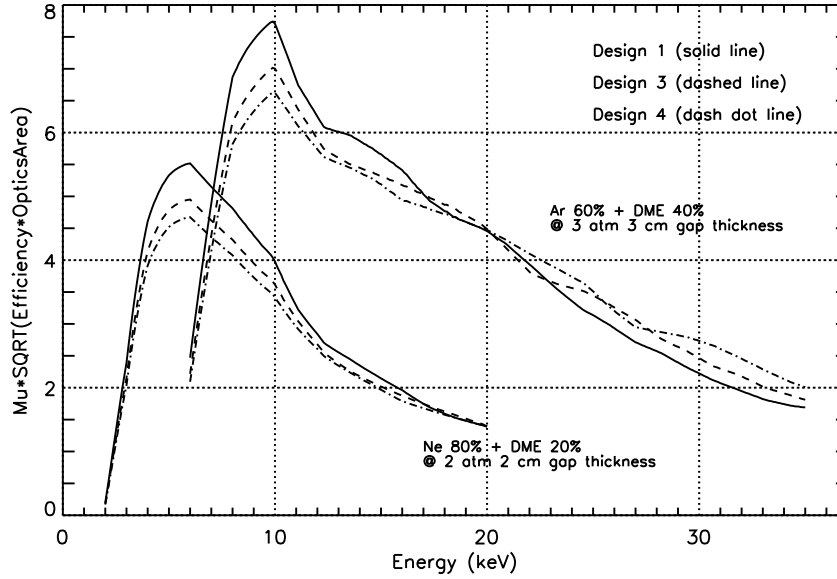


Figure 5. Sensibility factor $\mu\sqrt{\epsilon A}$ for SIMBOL-X designs considered for Ne 80% + DME 20% at 2 atm pressure and 2 cm gap thickness and 3 atm 3 cm Ar 60% + DME 40%.

3.1. Optics integration

We report now the performance that could be reached placing MPGC at focus of SIMBOL-X optics. We concentrate our attention on a mixture of Ar 60% + DME 40% at 3 atm pressure and 3 cm gap thickness, as the best choice for exploring polarimetry in hard X-rays.

In fig. 5 we report $\mu\sqrt{\epsilon A}$ factor for this mixture and three SIMBOL-X design considered: for comparison, the sensitivity of a Neon based mixture is plotted. Among three different SIMBOL-X versions analyzed, the first one is preferable because of larger area below 20 keV.

The Argon based mixture allows a polarization measurement between 6 and 30 keV: the minimum detectable polarization reached placing in the focus of design 1 SIMBOL-X optics is plotted in fig. 6 for different observation times.

The high sensitivity and large energy band would allow for a spectral study of polarization in this energy range: we present now this analysis for three sources, from which high polarization is expected.

3.1.1. Cyclotron lines in pulsating transient X0115+63 spectrum

The spectrum of pulsating transient X0115+63 shows 4 cyclotron resonant scattering feature¹² at 12.7, 24.2, 35.7 and 49.5 keV, which are expected to be nearly completely polarized.¹³ An Argon based MPGC could perform polarization measure till the second line: in fig. 7 we reported expected MDP in three energy bands, 11-14 keV, 14-22 keV and 22-27 keV.

3.1.2. Polarization measurement of Vela X-1 pulse

Phase and energy-dependent polarization analysis for eclipsing high mass X-ray pulsar Vela X-1 would be of great interest to discriminate among different models which on the other hand give similar spectra: variable polarization $>10\%$ is expected.¹³ Basing on spectrum studies reported in ref. 14, we evaluate MDP for first minimum and first part of the ascent edge of the first pulse peak: results are reported in tab. 4. Thanks to

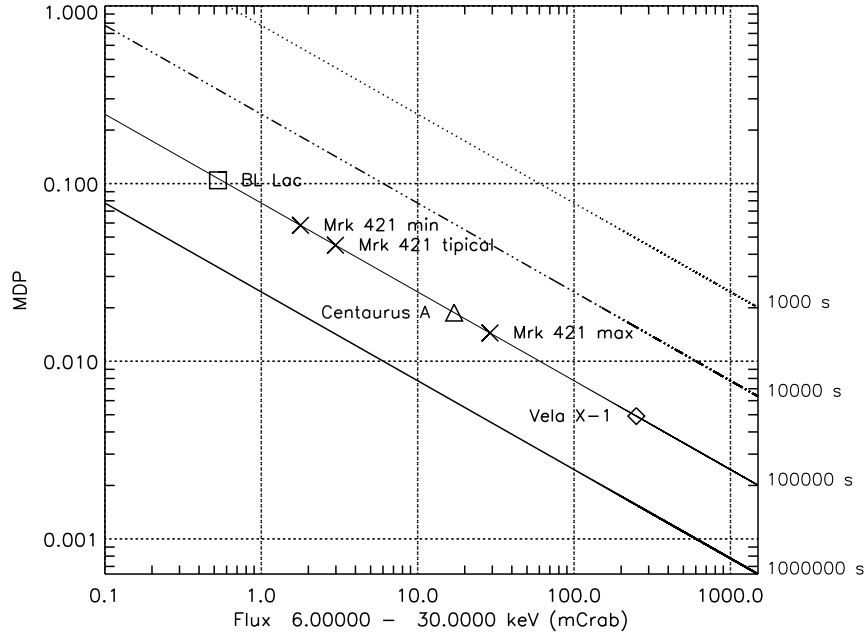


Figure 6. Minimum detectable polarization vs flux (expressed in mCrab) in the band 6-30 keV reached placing in the focus of the SIMBOL-X optics (design 1) a MPGC filled with Argon based mixture. On the right the observation time in seconds is reported: a few of representative sources are shown assuming an observation time of 10^5 sec.

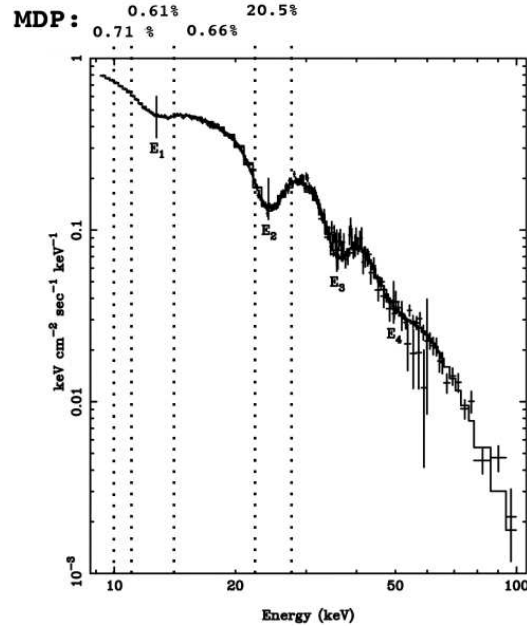


Figure 7. Minimum detectable polarization reached for pulsating transient X0115+63. Cyclotron resonant scattering feature at 12.7, 24.2, 35.7 and 49.5 keV are expected to be nearly completely polarized. Polarization measurement above 27 keV are not feasible with configuration considered. An observation time of 10^5 sec is assumed (adapted from ref. 12).

the large source flux, very accurate polarization measurements are possible, allowing the detailed description of neutron star magnetosphere and the determination of spin axis and magnetic field geometry.

Table 4. MDP estimate of first minimum and first part of the ascent edge of the first pulse peak of Vela X-1 spectrum with an observation time of 10^5 sec.

Energy band (keV)	MDP for first minimum	MDP for first part of the ascent edge of the first peak
6-15	0.0068	0.0063
15-30	0.0162	0.0144
6-10	0.0088	0.0082
10-15	0.0096	0.0088
15-20	0.0171	0.0151
20-30	0.0507	0.0447

3.1.3. BL Lacertae objects: Markarian 501

Markarian 501 is one of the closest ($z=0.034$) and brightest at all wavelengths BL Lacertae objects. Its spectrum in X-ray can be fitted with a power law of spectral index $\alpha \sim 1.5$ and can be explained with Synchrotron Self Compton emission, which should be polarized at a level $\geq 10\%$.^{15,16} The measure of polarization can enlighten the physics of the jet: in tab. 5 we reported the MDP evaluated in two energy bands for 3 atm 3 cm Argon based mixture and SIMBOL-X optics.

Table 5. MDP estimate for Mrk 501 at low state (power law spectral index ~ 1.5) for an observation time of 10^5 sec.

Energy band (keV)	Min	Max	Outburst
6-15	0.0412	0.0174	0.0201
15-30	0.1068	0.0450	0.0433

4. CONCLUSIONS

We calculated sensitivity to hard X-ray polarization of Micropattern Gas Chamber, assuming Neon and Argon based mixures at different pressure and absorption gap thickness. Results demonstrate that current instruments filled with Argon + DME mixture can perform astronomical sources polarimetry up till ~ 30 keV, allowing the study of compact galactic and extragalactic sources like X-ray pulsar or blazar. For bright sources, spectral dependence of polarization could be measured in a day of observation time, opening a new view on studies of high energy process in astrophysics.

4.1. Acknowledgments

This research is sponsored by INFN, INAF and ASI.

REFERENCES

1. G. Pareschi and V. Cotroneo, “Soft (0.1 - 10 keV) and hard (> 10 keV) x-ray multilayer mirrors for the XEUS astronomical mission,” in *SPIE Proc.*, **5168**, p. 53, 2003.
2. G. Pareschi, V. Cotroneo, D. Spiga, D. Vernani, M. Barbera, M. A. Artale, A. Collura, S. Varisco, G. Grisoni, G. Valsecchi, and B. Negri, “Astronomical soft x-ray mirrors reflectivity enhancement by multilayer coatings with carbon overcoating,” in *SPIE Proc.*, **5488**, p. 481, 2004.

3. M. C. Weisskopf, G. G. Cohen, H. L. Kestenbaum, K. S. Long, R. Novick, and R. S. Wolff, "Measurement of the X-ray polarization of the Crab Nebula," *The Astrophysical Journal* **208**, pp. L125–L128, Sept. 1976.
4. P. E. Kaaret, R. Novick, C. Martin, T. Hamilton, R. Sunyaev, I. Y. Lapshov, E. H. Silver, M. C. Weisskopf, R. F. Elsner, G. A. Chanan, G. Manzo, E. Costa, G. W. Fraser, and G. C. Perola, "SXP: a focal plane stellar x-ray polarimeter for the Spectrum-X-Gamma mission," in *Proc. SPIE Vol. 1160, p. 587-0, X-Ray/EUV Optics for Astronomy and Microscopy*, Richard B. Hoover; Ed., R. B. Hoover, ed., pp. 587–0, July 1989.
5. E. Costa, P. Soffitta, R. Bellazzini, A. Brez, N. Lumb, and G. Spandre, "An efficient photoelectric X-ray polarimeter for the study of black holes and neutron stars," *Nature* **411**, pp. 662–665, June 2001.
6. R. Bellazzini, G. Spandre, M. Minuti, L. Baldini, A. Brez, F. Cavalca, L. Latronico, N. Omodei, M. M. Massai, C. Sgró, E. Costa, P. Soffitta, F. Krummenacher, and R. de Oliveira, "First light from a very large area pixel array for high-throughput x-ray polarimetry," in *SPIE Proc.*, **6266**, 2006.
7. R. Bellazzini, L. Baldini, A. Brez, F. Cavalca, L. Latronico, N. Omodei, M. M. Massai, M. Minuti, M. Razzano, C. Sgró, G. Spandre, E. Costa, and P. Soffitta, "Gas pixel detectors for high-sensitivity x-ray polarimetry," in *SPIE Proc.*, **6266**, 2006.
8. R. Bellazzini, L. Baldini, A. Brez, E. Costa, L. Latronico, N. Omodei, P. Soffitta, and G. Spandre, "A photoelectric polarimeter based on a Micropattern Gas Detector for X-ray astronomy," *Nuclear Instruments & Methods in Physics Research* **510**, pp. 176–184, 2003.
9. J. J. Yeh, *Atomic Calculation of Photoionization Cross-Sections and Asymmetry Parameters*, Gordon and Breach Science Publishers, 1993.
10. M. O. Krause, "Atomic radiative and radiationless yields for K and L shells," *Journal of Physical and Chemical Reference Data* **8**, p. 307, 1979.
11. R. Bellazzini, L. Baldini, F. Bitti, A. Brez, F. Cavalca, L. Latronico, M. M. Massai, N. Omodei, M. Pinchera, C. Sgró, G. Spandre, E. Costa, P. Soffitta, G. D. Persio, M. Feroci, F. Muleri, L. Pacciani, A. Rubini, E. Morelli, G. Matt, and G. C. Perola, "A photoelectric polarimeter for XEUS: a new window in x-ray sky," in *SPIE Proc.*, **6266**, 2006.
12. A. Santangelo, A. Segreto, S. Giarrusso, D. dal Fiume, M. Orlandini, A. N. Parmar, T. Oosterbroek, T. Bulik, T. Mihara, S. Campana, G. L. Israel, and L. Stella, "A BEPOSAX Study of the Pulsating Transient X0115+63: The First X-Ray Spectrum with Four Cyclotron Harmonic Features," *The Astrophysical Journal* **523**, pp. L85–L88, Sept. 1999.
13. Meszaros, P. and Novick, R. and Szentgyorgyi, A. and Chanan, G. A. and Weisskopf, M. C., "Astrophysical implications and observational prospects of X-ray polarimetry," *The Astrophysical Journal* **324**, pp. 1056–1067, Jan 1988.
14. M. O. A. La Barbera, A. Santangelo and A. Segreto, "A pulse phase-dependent spectroscopic study of vela x-1 in the 8-100 keV band," *Astronomy & Astrophysics* **400**, pp. 993–1005, 2003.
15. J. Poutanen, "Relativistic jets in blazars: Polarization of radiation," *The Astrophysical Journal* **92**, pp. 607–609, June 1994.
16. A. Celotti and G. Matt, "Polarization Properties of Synchrotron Self-Compton Emission," *Monthly Notices of Royal Astronomical Society* **268**, p. 451, May 1994.